Comparative Study of pNaSS and pVBP on Titanium: Protein Adsorption, Cell Adhesion, and Bacterial Colonization

M. Lam[1,2]; V. Humblot[3], C. Falentin-Daudré[1*]

1- Biomaterial engineering and surface treatments (BEST), CB3S, Sorbonne Paris Nord University, Institut Galilée, 99 avenue JB Clément, 93430 Villetaneuse, France

2-Laboratoire de Physicochimie des Polymères et des Interfaces (LPPI), I-Mat, CY Cergy Paris Université, 95000 Neuville sur Oise, France

2- Université Marie et Louis Pasteur, CNRS, Institut FEMTO-ST (UMR 6174), F-25000 Besançon, France

*Corresponding author: falentin-daudre@univ-paris13.fr

Abstract:
This study examines how grafted polymers on titanium surfaces drive biological processes, focusing on the role of pre-adsorbed proteins in modulating cell and bacterial behavior. Here, pre-adsorbed proteins are used to mimic the initial physiological response post-implantation, not as a pre-coating strategy. Previous studies have shown that grafted poly(styrene sodium sulfonate) (pNaSS) enhances fibroblast (L929) adhesion, while poly(vinylbenzyl phosphonic acid) (pVBP) improves MC3T3 pre- osteoblast cells' osseointegration. Enhanced adhesion of fibronectin and fibrinogen on grafted surfaces, attributed to increased wettability, provides an organic matrix that promotes cell adhesion and favorable morphology. Bacterial adhesion of *S. aureus* was significantly reduced on pNaSS and pVBP-grafted surfaces (by 70% and 80%, respectively), as quantified by CFU assays.

These results highlight the specificity of biological responses based on surface modifications, protein type and bacterial strain.

The findings deepen understanding of how polymer grafting influences titanium's biological performance and guide its applications. They help address responses to questions like: Which cells should be targeted? Which proteins are key to these interactions? These insights enable tailoring biomaterial surfaces to specific clinical needs.

Key words: Titanium, biocompatibility, grafting, polymers, bacterial assay

Introduction:

Titanium-based materials are widely recognized as materials of choice in biomedical applications, particularly in orthopedics and dental implants, due to their excellent mechanical properties, corrosion resistance, and biocompatibility [1][2][3]. The inherent ability of titanium surfaces to promote osseointegration dates back to the 1980s with Brånemark's work [4]. While conducting an experiment, he observed that the titanium forceps he used had fused with the rabbit bone, leading to the concept of osseointegration.

Since then, the direct structural and functional connection between bone and modified titanium and its alloy implants has been extensively documented [5][6][7]. This compatibility is largely attributed to the titanium oxide layer that forms naturally on the surface, facilitating cell adhesion and bone formation [3].

It is well established that implant integration within the body is a complex, multifactorial process involving numerous biological molecules, such as extracellular matrix (ECM) proteins and immune cells [8]. A key early event in this process is the adsorption of soluble macromolecules like proteins onto the implant surface, which guides biological responses, including cell adhesion, proliferation, and bacterial attachment [9][10][11]. These interactions are significantly influenced by surface properties such as surface energy, roughness, surface charge, and chemical composition [12][13]. The ECM plays a central role by structurally supporting cells and regulating their behavior via biochemical cues. Key proteins like collagen, fibronectin, and laminin contain adhesion motifs that engage integrins, guiding cell attachment, survival, and differentiation [14]. These responses are also affected by environmental factors and the chemical nature of protein functional groups ($–COOH$, $–NH_2$, $–CH_3$) [15]. During the initial host response, a foreign body reaction (FBR) occurs, heavily influenced by protein adsorption. Material properties affect protein conformation and function, ultimately shaping how cells interact with the surface.

Among these proteins, fibronectin (Fn) and fibrinogen (Fg) are of particular interest due to their fibrillar structures and distinct biological roles. Fibronectin, a key ECM component, mediates cell attachment, while fibrinogen, primarily found in blood, contributes to clot formation and inflammation [16].

In the last decade, advancements in surface modification techniques have demonstrated that the biological performance of polymers or metallic substrates can be further enhanced through the grafting of bioactive polymers such as pNaSS (poly(sodium styrene sulfonate)) [17][18] or pVBP(poly(vinylbenzyl phosphonic acid)) [19][20][21], bearing sulfonate ($-SO_3^-$) and phosphonate ($-PO_3^{2-}$) groups, respectively. The UV-induced "grafting from" technique has been extensively studied as it allows uniform polymer coverage and covalent surface attachment [22][23]. These anionic polymers have the potential to significantly improve cell adhesion, proliferation and differentiation [19]. Unlike cationic or zwitterionic polymers, which may limit biocompatibility or protein interactions, these anionic polymers promote selective protein adsorption and subsequent cell adhesion, key steps for the integration of implants such as titanium into biological tissues. Numerous surface-grafted polymers have been explored for improving implant biointegration, offering specific properties such as antifouling, antibacterial effects, or tissue selectivity [24][25]. In this study, we deliberately selected pNaSS and pVBP, which share a similar aromatic backbone but differ in their anionic pendant groups (sulfonate vs. phosphonate), allowing a focused comparison of how charge chemistry influences protein adsorption and biological responses. pNaSS has been reported to enhance fibroblast (L929) adhesion and proliferation [17–19], whereas pVBP promotes pre-osteoblast (MC3T3) adhesion, osteogenic differentiation, and exhibits strong affinity for bone mineral phases [19,20,26]. Investigating these polymers thus provides mechanistic insight relevant to designing bioactive implant surfaces.

Recent research also highlights that grafted polymers may influence the behavior of extracellular matrix proteins, particularly fibronectin [10][27][28]. The grafted polymers confer specific chemical functionalities and introduce negative surface charges, which influence protein–surface interactions through mechanisms such as electrostatic forces, hydrogen bonding, hydrophobic interactions, and van der Waals forces [29].

In this study, poly(sodium styrene sulfonate) (pNaSS) and poly(vinylbenzyl phosphonic acid) (pVBP) were grafted onto titanium surfaces to investigate the role of the protein layer that forms immediately upon implantation. We focus on how the anionic pendant groups influence the adsorption and conformation of fibronectin and fibrinogen, proteins that were pre-adsorbed to mimic the early *in vivo* environment, and how these layers affect subsequent cellular and bacterial responses. Cytocompatibility, cell adhesion, and bacterial colonization with *Staphylococcus aureus*, a common pathogen in titanium implant infections, were evaluated to compare the effects of sulfonates and phosphonate functionalities. Titanium was selected as a clinically relevant model substrate to isolate the impact of surface chemistry. The findings aim to inform the design of next- generation implants with improved bioactivity and resistance to infection.

Materials & Methods:

- ### Material

Grade 2, commercially pure Ti disks (10 mm; ≈ 1 mm thickness) purchased from Goodfellow (supplier set in Lille, France); *Monomers:* (4-Vinylbenzyl) phosphonic acid (VBP) powder (from Specific Polymers); sodium styrene sulfonate powder (Sigma Aldrich) was purified using a well-elaborated protocol with alternate steps of hot and cold Büchner filtrations [23][30]. The purified product is stored at 4° C before use [17][18][23]; Polymerization initiator 2,2′ -azobis(2-methylpropionitrile) (AIBN), was refined by a recrystallization process at 30° C for 1 h. *Proteins:* Soluble fibronectin & fibrinogen (Sigma Aldrich).

- **Surface characterization methods**

Scanning electron microscopy coupled to Peltier module: Adhered cells' morphology and spreading over the Ti surfaces after the different surface treatment were analyzed under using a scanning electron microscope – SEM (Hitachi TM3000). The Peltier complement allowed high quality images minimizing the condensation effect due to the sample humidity.

Fourier Transform Infrared Spectroscopy (FTIR – ATR): ATR-FTIR was chosen for its ability to detect adsorbed proteins non-destructively by identifying characteristic protein bands (amide I and II). Measurements were done with a PerkinElmer Spectrum Two using a diamond ATR crystal, which provides a penetration depth of about 0.5–2 µm. Spectra were recorded at 4 cm^{-1} resolution with 128 scans between 600 and 4000 cm^{-1} and then analysed.

Contact angle measurements: The wettability of the titanium surfaces was accessed using a contact angle measuring device (DSA10, KRUSS GmbH) following the sessile droplet method. A water droplet volume of 2 μL is deposed onto the surface and after equilibrium, and the contact angle is measured based on Young-Lapres fitting model. The measurements are triplicated for each condition.

Titanium surfaces preparation:

Titanium surfaces were polished (500 and 1200 grit *SiC* papers), ultrasonically cleaned with acetone, cyclohexane, isopropanol, and distilled water, then etched in Kroll's reagent for one minute (2% hydrofluoric acid, 10% nitric acid, 88% distilled water). After rinsing in distilled water, the surfaces were dried at 50° C. The Ti substrates were then oxidized for 4 minutes in a 50:50 (v/v) ratio mixture of concentrated sulfuric acid (H_2SO_4) and hydrogen peroxide (H_2O_2, 30%) to activate the surface, followed by rinsing with distilled water [19].

- **Grafting**

To graft **pNaSS** or **pVBP** onto Ti surfaces, solutions were prepared by dissolving NaSS in 20 mL of dH_2O or VBP in 4 mL of DMSO with 2% AIBN initiator. After degassing each solution with argon for 30 minutes, the oxidized Ti substrates were added. Immersed in NaSS/dH_2O [17][18] or VBP/DMSO solutions [19], the surfaces were irradiated with UV light (365 nm, 160 mW/cm^2) for 2 hours at room temperature with stirring. The grafted surfaces were then either washed with dH_2O or DMSO/methanol (50:50 v/v), then methanol for 48 hours, and dried overnight at 37° C.

Biological assays:

For biological experiments, samples were cleaned in sterile phosphate-buffered saline solution (PBS) for 6 hours and sterilized under UV irradiation (254 nm) for 15 minutes per side in a laminar flow hood.

- **Protein adsorption**

Human Fibronectin (Fn) and fibrinogen (Fg) (Sigma Aldrich) were diluted in sterile PBS to a of 0.02 mg/mL and 0.10 mg/mL, respectively [(31)(32)] and gently stirred. For adsorption, 1 mL of the protein solution was added to each surface and incubated at 37° C for 1 h (Fn) or 2 h (Fg) [(16)(33(34)(35)]. Unadsorbed proteins were removed by two PBS rinses.

- **Cell culture**

L929 Mouse fibroblasts (ATCC) and MC3T3 pre-osteoblasts (ATCC) cell lines were used for cytotoxicity, biocompatibility, mineralization, and morphology assessments.

Cell seeding: Fibroblasts were suspended in Dulbecco's Modified Eagle Medium (DMEM, Gibco), used as the culture medium for this cell type, while MC3T3 pre-osteoblasts were suspended in Minimum Essential Medium Alpha (α-MEM, Gibco), which is appropriate for their growth. Cells were seeded onto the samples in multi-well plates at 37° C with 5% CO_2 (5×10^4 cells/mL/well). Incubation times varied depending on the assay.

Assessment of cytotoxicity – MTT test: Cell viability was assessed through the measurement of the mitochondrial dehydrogenase activity. A tetrazolium salt solution (3-(4,5-dimethylthiazol-2-yl)-2,5- diphenyltetrazolium bromide, MTT, Sigma) was prepared at 5 mg/mL in DMEM without phenol red, forming purple formazan crystals upon reaction with live cells.

After incubation and washing, 100 μL of MTT solution mixed with 400 μL of DMEM is added to each surface and incubated for 4 hours at 37° C in the dark. Following this, the samples are rinsed, and decomplexation is performed by adding 350 μL of dimethyl sulfoxide (DMSO) to dissolve the formazan crystals. The absorbance was then read at 570 nm (ELx800, BioTek). Cell viability was calculated from the optical densities (OD) using the formula:

Equation 1: Viability rate calculation

$$\boldsymbol{Vr}(\%) = \frac{\boldsymbol{DOs} - \boldsymbol{DOn}}{\boldsymbol{DOp} - \boldsymbol{DOn}} * \mathbf{100}$$

DO_s: Surface optical density
DO_p: Positive control optical density
DO_n: Negative control optical density

Evaluation of cell morphology: Cells were incubated on surfaces for 24 hours, 3 days, and 7 days. After each period, surfaces were rinsed with PBS, fixed with 400 μL of 4% formaldehyde for 30 minutes at 4° C, washed with ultrapure water, and stored.

Alizarin Red S staining assay: Calcium deposition was quantified using Alizarin Red S staining. Samples were rinsed with PBS, fixed in 70% ethanol at 4° C for 1 hour, then air-dried. They were stained with 1 mL of 40 mM Alizarin Red S solution for 1 hour at room temperature, protected from light. Excess dye was removed by PBS washes. The bound dye was then extracted using 1 mL of 1% cetylpyridinium chloride (CTP) solution for 15 minutes. Absorbance was measured at 570 nm using a spectrophotometer (ELx800, BioTek), and calcium content was determined using a calibration curve. One mole of Alizarin Red S was considered to bind two moles of calcium [36].

- **Bacterial assays:**

Microbiological experiments were conducted using *Staphylococcus aureus* strains *(S. aureus ATTC 25923).*

Oxidized titanium	Ti_Ox	Etching + oxidation
pNaSS grafted titanium	Ti_pNaSS	UV-induced polymerization
pVBP grafted titanium	Ti_pVBP	UV-induced polymerization

The bacterial inoculum was prepared first by growing a solid culture on agar (15 g/L) supplemented with Mueller-Hinton (MH) medium (21 g/L) on Petri dishes, incubated overnight at 37° C. Next, a liquid pre-culture was prepared by inoculating a single *S. aureus* colony into MH medium and incubating for 18 hours at 37° C under stirring (90 rpm). 1 mL of exponentially growing *S. aureus* cells were harvested by centrifugation (5000 g, 5 minutes, Room Temperature). The supernatant was discarded and replaced with sterile PBS. After vortexing the previous aliquot, a second centrifugation was performed, and the bacterial pellet was resuspended in 1 mL of fresh sterile PBS. From this suspension, a bacterial solution of defined concentration was prepared by diluting the original suspension with PBS. The bacterial suspension was adjusted to an optical density (OD) of 0.01 at 620 nm, corresponding to 5×10^6 CFU/mL^{-1}.

Next, 1 mL of the diluted bacterial suspension was added to each titanium surface in 24 well-plates and incubated for 3 hours at 37 °C under stirring. After incubation, the surfaces were removed from the solution, briefly drained on absorbent paper, and individually placed into small containers holding 2 mL of PBS. These containers were then placed in an ultrasonic bath for 3 minutes to detach bacteria adhered to the Ti surfaces.

The resulting solution was collected and serially diluted 10-fold (C and C/10). For each specimen, 50 μL of both the undiluted and diluted solutions were spread onto Petri dishes containing a mixture of sterilized agar powder and Mueller-Hinton medium. Spreading was performed using an automatic seeder (EasySpiral, Interscience). Plates were incubated overnight at 37 °C, and colony-forming units (CFUs) were enumerated using an automatic colony counter (Scan 300, Interscience). Results were expressed as the number of attached and cultivable bacterial cells on the different surfaces, reported as CFU/mL^{-1}.

- **Statistical analysis**

Statistical analyses were performed using one-way ANOVA followed by Tukey's post-hoc test to assess significant differences between groups. For each experiment, at least 3 samples were considered.

Table 1 : Titanium and the different surfaces treatment and denominations

Samples	Denomination	Chemical treatments	Grafted functions
Non grafted titanium	Ti_NG	Etching (Kroll reagent)	

Result and discussion

1. Grafting of polymers onto titanium surfaces

For both polymers, the protocol relies on a “grafting from” mechanism, where the polymer chains grow from a radical species created on the surface, as illustrated in Figure 1. To achieve this, titanium surfaces undergo an oxidation step in an acidic mixture prior to any grafting treatment. This step facilitates the formation of functional groups on the surface, specifically hydroxyl groups (-OH). Under UV irradiation and in solution, these hydroxyl groups generate oxygen radicals, which initiate polymer chain growth.[s17-19]

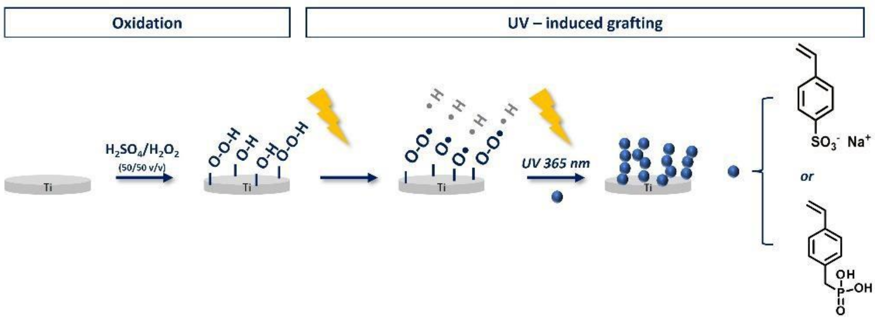

Figure 1 : Schematic representation of the titanium surface oiidation and VV-induced polymerization steps for the grafting of pNaSS and pVBP grafting in solution, H_2O or DMSO, respectively.

The follow-up of the Ti surface treatment steps is straightforward using surface characterization tools. The FTIR spectrum of Ti_NG (Figure 2) showed no specific vibration band associated with the bare surface. Once oxidized, a weak feature appeared at 3675 cm^{-1} attributed to free -OH groups. After grafting, as indicated by the arrows, new bands appeared, associated with the sulfonate or phosphonate groups. The bands at 1010 cm^{-1}, 1049 cm^{-1}, and 1129 cm^{-1} are attributed to sulfonate while those at 933 cm^{-1}, 985 cm^{-1}, 1253 cm^{-1}, and 1509 cm^{-1} are attributed to the phosphonates. The C=C stretching band for aromatic rings is typically observed around 1600 cm^{-1} for both polymers but appears less clearly in the pNaSS spectrum. These results are consistent with data from literature [19][37].

Additionally, the polymers induced a change in surface wettability. Ti_NG showed an average apparent contact angle of 57.5° ± 0.2, while the contact angles for the different surface treatments were measured as 36° ± 4.9, 16.5° ± 5.8, and 50.4° ± 3.8 for oxidized, pNaSS grafted and pVBP grafted surfaces, respectively [19]. The change in surface hydrophilicity indicates that the surfaces underwent effective modifications with pNaSS and pVBP.

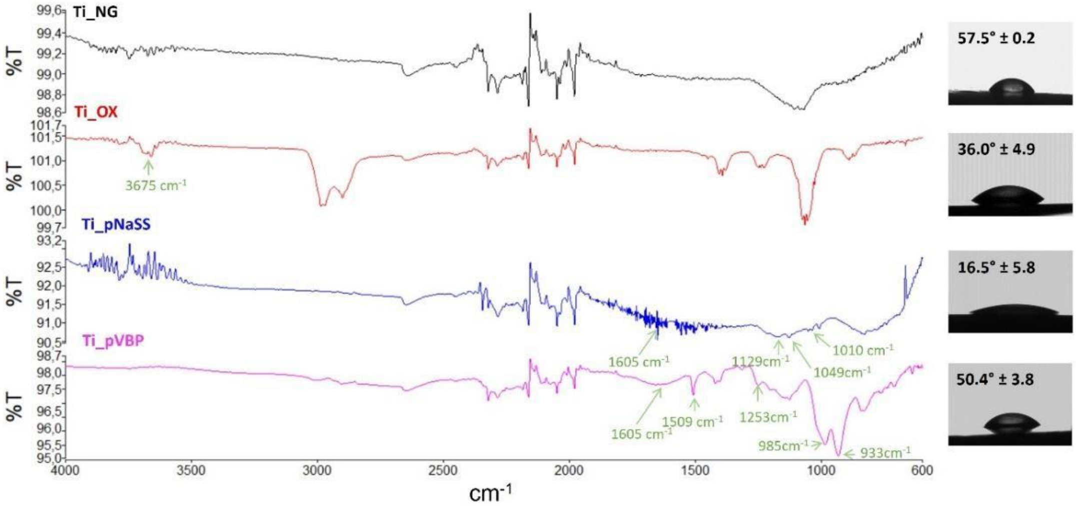

Figure 2 : FTIR spectra of the non-grafted and modified titanium surfaces with their resulting wettability evaluated by the measurement of the apparent water contact angles.

The next sections will be fully dedicated to the study of surface-biological fluids interactions.

2. Comparing the bioreactivity of two surface modifications

2.1. Protein adsorption on grafted surfaces

Fibronectin (Fn) and fibrinogen (Fg), two proteins characterized by their fibrillar structures in their native conformations and their distinct physiological roles were pre-adsorbed onto the surfaces to mimic the natural protein layer formed after implantation, aiming to replicate physiological conditions.

The concentrations used (0.02 mg/mL for Fn and 0.10 mg/mL for Fg) are lower than physiological levels to ensure formation of a thin, uniform protein layer under experimentally controlled conditions. This approach allows precise study of how surface modifications affect early protein– material interactions and subsequent biological responses.

The surface modifications brough by the grafting of pNaSS and pVBP are expected to alter protein adsorption behavior, thereby modulating downstream cell and microbial responses. Macroscopically, protein adsorption changed the surfaces' wettability from hydrophilic to hydrophobic with a clear increase in the contact angles (Figure 3). After adsorption, the protein layer seems to have taken over the overall wettability. Hypotheses related to surface/protein interactions could be formulated based on the results. Based on these findings, several hypotheses can be proposed regarding protein orientation and surface interactions. It is plausible that hydrophobic domains of the proteins are oriented outward, while hydrophilic regions interact with the polar functional groups of the grafted polymers [38]. Additionally, negative charges introduced by the sulfonate and phosphonate groups might have driven protein adsorption into monolayers or multilayers, for example [39].

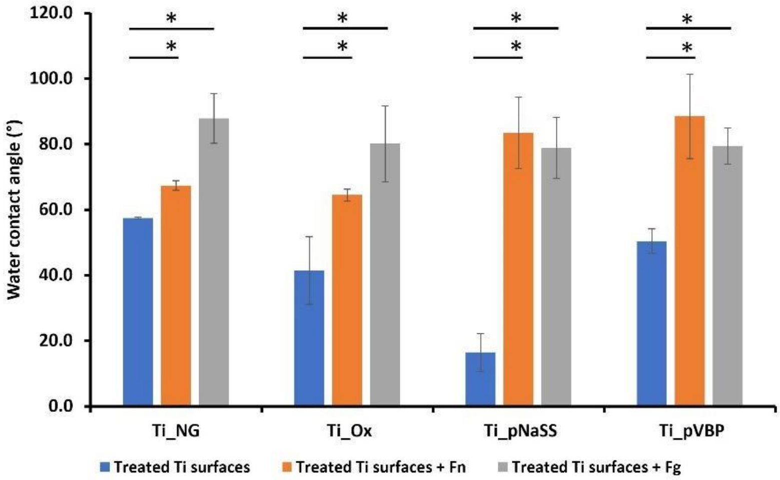

Figure 3 : Measurement of water contact angles after the deposition of a droplet of water on the different Ti substrates after fibronectin (1h) and fibrinogen (2h) adsorption ($p<0.05$)*

Protein adsorption over the surfaces is then effectively characterized by FT-IR spectroscopy, as evidenced by the appearance of two bands at 1650 cm^{-1} and 1550 cm^{-1}, corresponding to the peptide bond (NH-C=O) (Figure 4). The Amide I band, located at 1650 cm^{-1}, is primarily associated with C=O stretching vibrations and is directly related to the backbone conformation. The Amide II band, at 1550 cm^{-1}, arises from N-H bending vibrations and C-N stretching vibrations.

Interestingly, from a qualitative point of view, the intensity of the bands appears to be higher with Ti_pVBP in the fibronectin experiment (Fig.4a), whereas the opposite is observed in the fibrinogen experiment (Fig.4b). This could be attributed to several factors, such as a greater quantity of adsorbed protein, a larger surface coverage or a distinct organization of the adsorbed layer that exposes more peptide bonds. Deeper analyses are necessary to confirm this. Overall, pNaSS and pVBP interact differently with the same protein. Nevertheless, while these factors may explain the variations in intensity, our primary objective is to achieve a thin and controlled protein layer on the surface. By doing so, we aim to characterize the structural state and conformation of the protein after interaction with the modified surfaces, rather than simply maximizing adsorption.

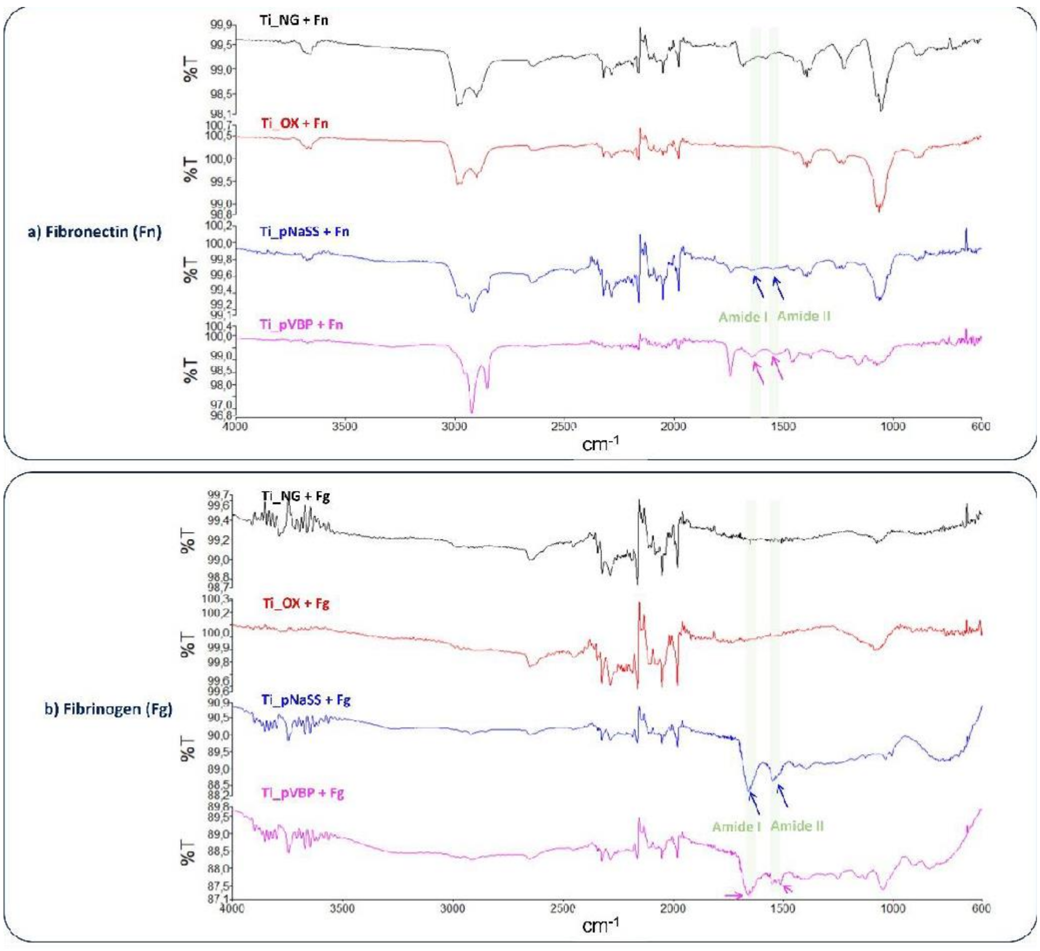

Figure 4 : FT-IR spectra of Ti substrates after (a) fibronectin adsorption and (b) fibrinogen adsorption.

Once the protein adsorption step was successfully characterized. The studies with cells and bacteria were carried out.

2.2. Cell culture

- **Viability – cytotoxicity**

Assessment of cytocompatibility is a key step in advancing any biological assay. An MTT assay was performed after 24 hours of cell seeding. The choice of L929 fibroblasts was made according to the ISO 10993 biomedical device regulation [(40)]. The test relies on the capacity of surface-adhered viable cells to convert MTT reagent into purple formazan crystals, reflecting the viability rates of cells on the surfaces.

The results, depicted in Figure 5, show that both polymers, once grafted, significantly improved viability rates compared to the initial non-grafted Ti, with viability rates of 96% and 77%, slightly higher for Ti_pNaSS. The ISO 10993-5 standard on in vitro cytotoxicity testing establishes that a material is considered cytotoxic if it reduces cell viability below 70% compared to a negative control. This threshold helps distinguish materials with significant toxic effects from those considered biocompatible. The significant differences observed between non-grafted and grafted Ti indicate that the grafted functionalities play a role in improving surface biocompatibility. These findings confirm that the grafted polymer effectively promotes fibroblast viability, making it a promising approach for enhancing biocompatibility.

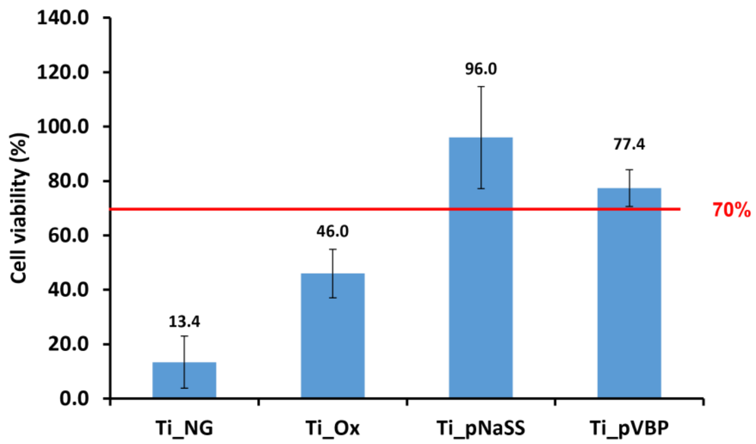

Figure 5 : MTT assay for viability rates of L929 fibroblast cells cultured on different titanium substrates for 24 hours (n=3). Viability rates on the y-aiis are calculated relative to a control well with no Ti substrate.

- **Cells organization and morphology**

Evidencing the way cells adhere and are organized on a surface provides deeper information on its suitability. Considering the potential use of titanium as bone repair material, it is necessary to control cell adhesion to optimize the following process. In the context of titanium use, MC3T3 pre-osteoblast cells were used in the following experiments. Figure 6 shows adhering cells to different surfaces at 1 hour and 4 hours incubation time with and without fibronectin. The SEM images of pre-osteoblast cells highlight the effects of both adsorbed fibronectin (Fn) and surface treatments. A general observation is that the concentration of cells per unit area is higher after 4 hours of incubation compared to 1 hour, which makes complete sense: the longer the cells incubate, the more time they have, to adhere (Figure 6).

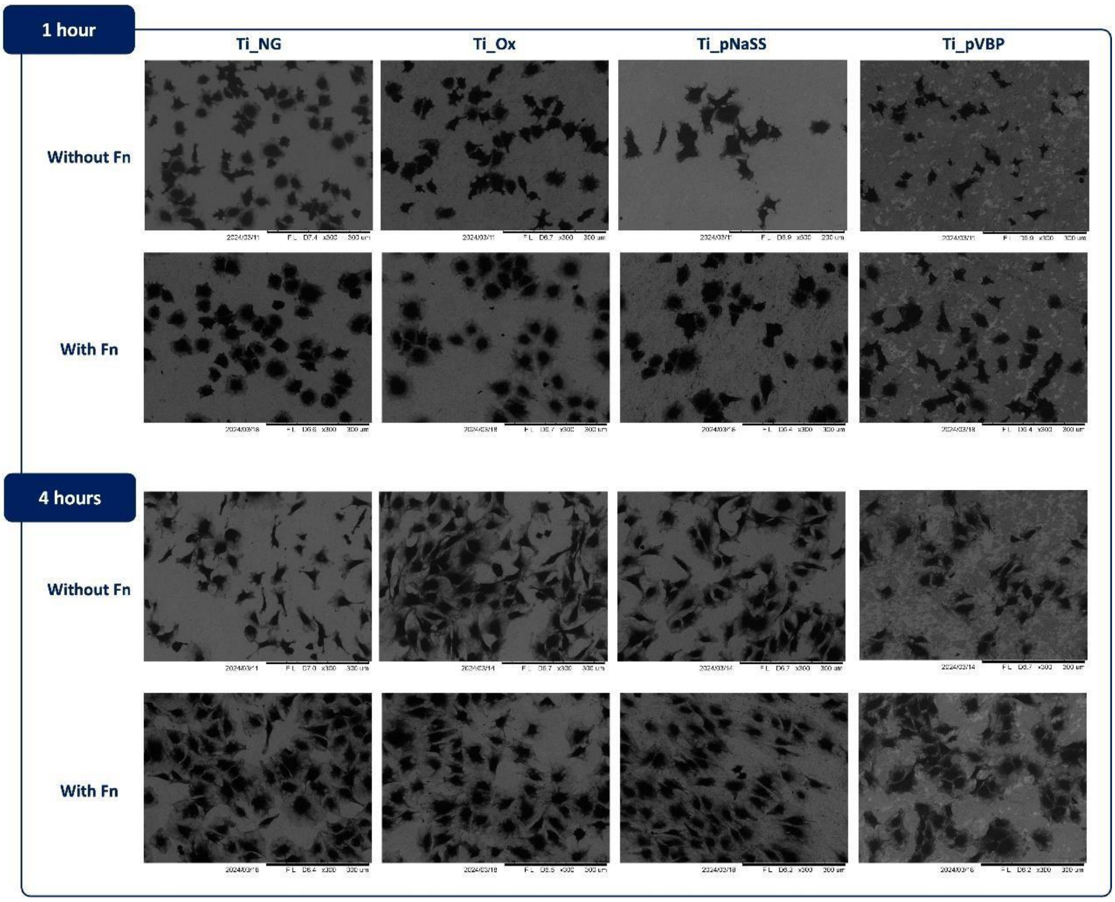

Figure 6 : SEM images of MC3T3 pre-osteoblasts fiied on different Ti substrates. Two parameters are investigated: the incubation time and the presence of adsorbed fibronectin.

A closer examination reveals differences between the surface treatment conditions. Without adsorbed fibronectin (Fn), cells preferentially adhere to Ti_NG and Ti_Ox surfaces compared to polymer-grafted surfaces. In the presence of fibronectin, the tendency is more balanced. However, differences in cell spreading can be observed. On Ti_NG and Ti_Ox, the cells are predominantly spherical, with some showing a cubic morphology. In contrast, on polymer-grafted titanium surfaces, individual cells appear to occupy a larger area with a more spread-out shape. In fact, proteins such as fibronectin and vitronectin strongly contribute to cell adhesion when in contact with pNaSS grafted surfaces [(34)]. Moreover, hydrophilic surfaces influence fibronectin binding, promoting greater adsorption to the surfaces and providing strong support for cell adhesion [(41)]. The spreading phenomenon is even more pronounced on Ti_pVBP, where cells exhibit a fusiform (spindle-like) shape. This result aligns with the fact that MC3T3 cells interact more favorably with phosphonate groups because of their bone-like apatite-induced ability [(42)].

The accuracy of these observations is confirmed when the study is extended to longer incubation times, 4 hours. On Ti_pVBP, the pre-osteoblasts are flakily embedded, whereas on the other surfaces, cells adhere and proliferate without any clear signs of specific organization. On Ti_pVBP, cells interact and self-assemble into organized structures, as seen in the SEM images. This observation is significant because, in the long run, effective bone tissue regeneration requires a well-organized initial cell layer.

These qualitative insights underscore the importance of surface-protein interactions in driving cell behavior and highlight the specificity of phosphonate groups toward bone cells compared to Ti_pNaSS.

- **Mineralization quantification : Alizarin red assay**

The differentiation of pre-osteoblast cells into mature osteoblasts is strongly influenced by the quality and composition of the substrate (19). As the last step of differentiation, the quantification of calcium production is relevant (43). Herein, we have studied the formation of calcium nodules by cells. Through a chelation process, the anthraquinone derivative reacts specifically with calcium cations to form a complex, resulting in a dark red stain.

As shown in Figure 7, a general increase in calcium concentration is observed over time, which is expected since longer incubation periods allow cells to produce more calcium. It is important to note that fibronectin was pre-adsorbed. But interestingly, compared to a previous study where no protein was involved, calcium levels were significantly different between a non-grafted Ti and a grafted one (19). This can be attributed to the adsorbed protein layer acting as a barrier between the titanium surface and the cells, thereby modifying their interaction with the substrate. This effect can moderate or even reduce the rate of osteoblast differentiation, suggesting a hindering influence. Given that fibronectin (Fn) may have a particular affinity for sulfonate groups, this could explain the significant increase observed between 21 and 28 days of incubation (44) while no variation is observed in the non- grafted and pVBP grafted groups.

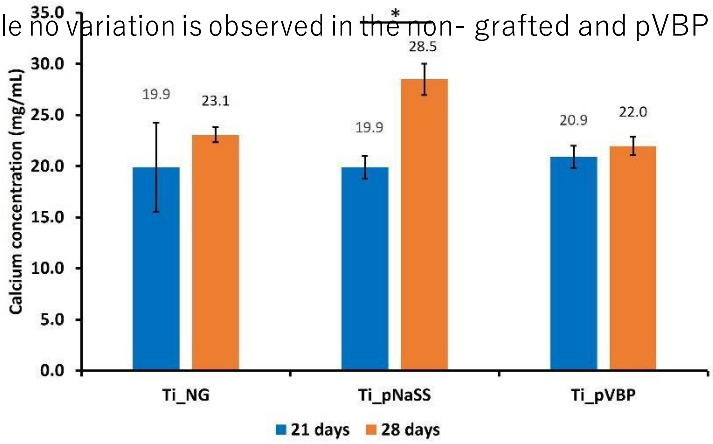

Figure 7 : Evaluation of the calcium rates produced by the cells after 21 days and 28 days of incubation with the alizarin red assay (p<0.05)*

In conclusion, this experiment underscores again the critical role of protein layers in shaping subsequent biological responses. It highlights their importance in studies focused on the interplay between surface properties and cell behavior, emphasizing that protein-material interactions should be carefully considered in the design and evaluation of biomaterials.

2.3. Antibacterial response

Biofilms are a major cause of implant failure due to their resistance to host defenses and antibiotics [45]. Beyond biocompatibility, material performance also depends on its ability to limit microbial growth. We therefore evaluated the bacterial inhibition of Ti surfaces, with and without protein adsorption, to assess the direct and indirect effects of grafted groups. Assays were performed with *Staphylococcus aureus*, a highly pathogenic strain (negatively charged) commonly involved in device-associated infections [46].

The blue histogram below (Figure 8) shows an increase in viable bacterial concentrations upon surface contact when grafted with either pNaSS or pVBP. These observations indicate that the biocompatibility of the grafting evidenced earlier is not solely dependent on the exposed surface groups. As seen with the yellow bars, the presence of adsorbed Fn has dropped the bacterial concentrations by nearly 70% on polymer-grafted titanium surfaces, with greater reductions on Ti_pVBP. This finding indicates that Fn adsorbs specifically and plays a crucial role in influencing *S. aureus* adhesion through its organization (fibrillar or globular) [35], which is dictated by surface interactions. Indeed, fibronectin contains integrin-binding domains that favor cell adhesion but might also inhibit bacterial attachment by physically or sterically blocking bacterial adhesins, showing a double functionality [47]. The phosphonate-coated titanium may influence the adsorption of fibronectin, promoting a specific conformation or orientation of the protein that better masks bacterial adhesion sites. Using AFM probing, Liamas *et al.* [48] demonstrated that fibronectin interactions with chemical functional groups, such as carboxylate or methyl groups, induced either an “end-on” or “side-on” conformation. These conformations either concealed or exposed fibronectin's binding sites, affecting its interactions with cells or bacteria.

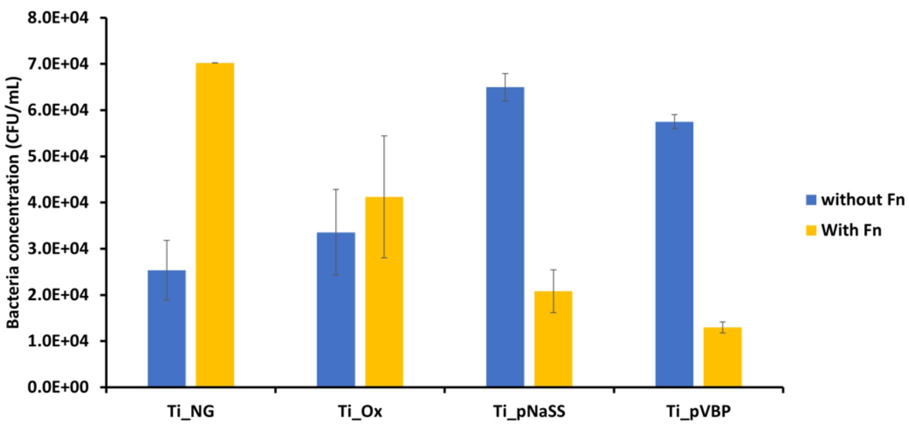

Figure 8: Enumeration of viable bacteria (CFV/mL) after overnight adsorption at 37°C on non-grafted and polymer-grafted Ti substrates.

Surface-protein interactions and protein-bacteria strain interactions are highly specific processes and cannot be generalized. Each scenario results in a unique response based on the specific protein and bacterial strain involved.

To illustrate this point, we tested the inhibition effect using fibrinogen (Fg). As shown in Figure 9, no bacterial inhibition was observed, and *S. Aureus* levels remained high regardless of surface treatment. Unlike fibronectin (Fn), Fibrinogen does significantly alter its structure or orientation upon adsorption and appears to interact similarly with both grafted and non-grafted surfaces. This lack of surface specificity likely explains the constant bacterial adhesion rate observed. Moreover, Fg does not seem to hinder *S. aureus* adhesion, possibly because it does not undergo major conformational changes and maintains a similar biological profile across surfaces. Supporting this, studies using *S. epidermidis* have shown minimal influence of pre-adsorbed fibrinogen on bacterial attachment. Additionally, *S. aureus* expresses MSCRAMMs that exhibit strong affinity for human fibrinogen [49], potentially facilitating rather than preventing adhesion. These findings highlight the importance of the specific

combination of grafted surface, adsorbed protein, and bacterial strain in determining the biological response.

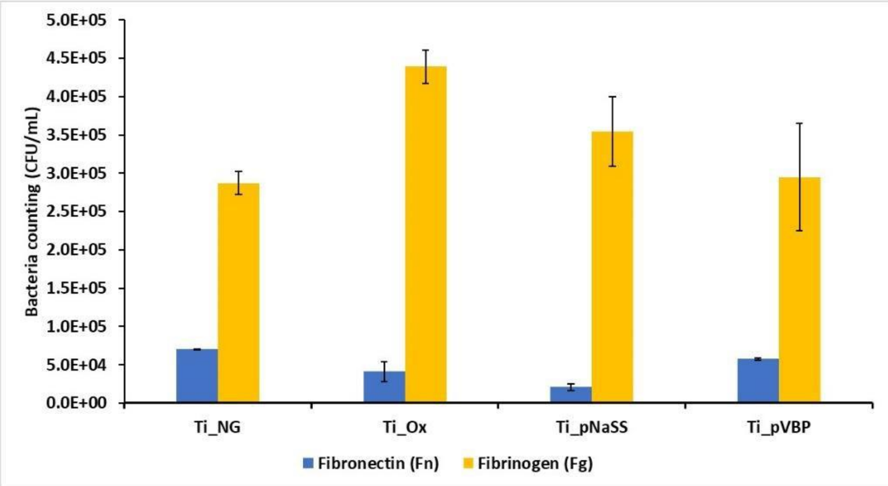

Figure 9 : Comparison of viable bacteria concentrations (CFV/mL) between Ti substrates with fibronectin or fibrinogen as the adsorbed protein layer.

Overall, this study aimed to demonstrate the specificity of one-to-one interactions between surface pendant groups, proteins, cells and bacteria. Although both grafted polymers are anionic and exhibit negative charges, their interactions with proteins and other biological molecules differ significantly, leading to variations in biological responses.

The multifactorial side of the biointegration process makes the study more complex when it comes to imitating what happens at the physiological scale. Here, the addition of a protein layer made the system more realistic. Even though the bioactive polymers are similar in their backbone structure and overall charge, they showed distinct affinities toward the same cell line, different interactions with proteins, and consequently, differing bacterial responses. These results support the existence of various types of interactions (chemical, electrostatic and hydrogen bonding) knowing that pNaSS is a salt and pVBP an acidic molecule.

These outcomes have led us to highlight one important point: despite similar physicochemical properties and structures, a given response is **highly dependent** on the nature of the molecules involved at the interface. Notably, **anti-bacterial adhesion is strongly influenced** by two main factors:

(1) the presence and nature of proteins and (2) their conformation and organization on the surface.

Conclusion

This study underscores the critical role of surface chemical groups and their influence on cell responses mediated by a protein layer. Using the same substrate, one was grafted with a salt-based polymer, the poly(styrene sodium sulfonate) and the other one with an acidic polymer, the poly(vinylbenzyl phosphonic acid), we have demonstrated that surface modifications significantly enhance biocompatibility, as reflected in increased cell viability rates compared to non-grafted counterparts. The protein layer, represented by fibronectin or fibrinogen, clearly impacted on the results. It not only provided an organic matrix that improved cell adhesion, as evidenced by SEM morphology analysis, but also influenced the antibacterial properties of the material. Our findings show that the *S. aureus* strain is sensitive to the nature of the protein: the presence of fibronectin on grafted surfaces reduced bacterial adhesion, whereas fibrinogen showed no significant effect, with respect to non-grafted surfaces. Overall, the results emphasize the specificity of one-to-one interactions and the necessity of considering protein layers in addition to surface properties. These outcomes pave the way for further research into surface characteristics such as charge, topography, and mechanical properties to gain a deeper understanding of the observed phenomena.

Bibliography

(1) Babaremu, K. O.; Jen, T.-C.; Oladijo, P. O.; Akinlabi, E. T. Mechanical, Corrosion Resistance Properties and Various Applications of Titanium and Its Alloys: A Review. Revue des composites et des matériaux avancés 2022, 32 (1), 11–16. DOI:10.18280/rcma.320102.

(2) Khorasani, A. M.; Goldberg, M.; Doeven, E. H.; Littlefair, G. Titanium in Biomedical Applications—Properties and Fabrication: A Review. Journal of Biomaterials and Tissue Engineering 2015, 5 (8), 593–619. DOI:10.1166/jbt.2015.1361.

(3) Hanawa, T. Biocompatibility of Titanium from the Viewpoint of Its Surface. Science and Technology of Advanced Materials 2022, 23 (1), 457–472. DOI:10.1080/14686996.2022.2106156.

(4) Carlsson, L.; Röstlund, T.; Albrektsson, B.; Albrektsson, T.; Brånemark, P.-I. Osseointegration of Titanium Implants. Acta Orthopaedica Scandinavica 1986, 57 (4), 285–289. DOI:10.3109/17453678608994393.

(5) Stich, T.; Alagboso, F.; Křenek, T.; Kovářík, T.; Alt, V.; Docheva, D. Implant‐bone‐interface: Reviewing the Impact of Titanium Surface Modifications on Osteogenic Processes in Vitro and in Vivo. Bioengineering & Translational Medicine 2021, 7 (1). DOI:10.1002/btm2.10239.

(6) Chen, C.-S.; Chang, J.-H.; Srimaneepong, V.; Wen, J.-Y.; Tung, O.-H.; Yang, C.-H.; Lin, H.-C.; Lee, T.-H.; Han, Y.; Huang, H.-H. Improving the in Vitro Cell Differentiation and in Vivo Osseointegration of Titanium Dental Implant through Oxygen Plasma Immersion Ion Implantation Treatment. Surface and Coatings Technology 2020, 399, 126125. DOI:10.1016/j.surfcoat.2020.126125.

(7) Lu, X.; Wu, Z.; Xu, K.; Wang, X.; Wang, S.; Qiu, H.; Li, X.; Chen, J. Multifunctional Coatings of Titanium Implants toward Promoting Osseointegration and Preventing Infection: Recent Developments. Frontiers in Bioengineering and Biotechnology 2021, 9. DOI:10.3389/fbioe.2021.783816.

(8) Anderson, J. M.; Rodriguez, A.; Chang, D. T. Foreign Body Reaction to Biomaterials. Seminars in Immunology 2008, 20(2), 86–100. DOI:10.1016/j.smim.2007.11.004.

(9) Rahmati, M.; Silva, E. A.; Reseland, J. E.; A. Heyward, C.; Haugen, H. J. Biological Responses to Physicochemical Properties of Biomaterial Surface. Chemical Society Reviews 2020, 49 (15), 5178–5224. DOI:10.1039/d0cs00103a.

(10) Parisi, L.; Toffoli, A.; Ghezzi, B.; Mozzoni, B.; Lumetti, S.; Macaluso, G. M. A Glance on the Role of Fibronectin in Controlling Cell Response at Biomaterial Interface. Japanese Dental Science Review 2020, 56 (1), 50–55. DOI:10.1016/j.jdsr.2019.11.002.

(11) Kreve, S.; Reis, A. C. Bacterial Adhesion to Biomaterials: What Regulates This Attachment? A Review. Japanese Dental Science Review 2021, 57, 85–96. DOI:10.1016/j.jdsr.2021.05.003. (12)Barberi, J.; Spriano, S. Titanium and Protein Adsorption: An Overview of Mechanisms and Effects of Surface Features. Materials 2021, 14 (7), 1590. DOI:10.3390/ma14071590. (13)Wang, K.; Zhou, C.; Hong, Y.; Zhang, X. A Review of

Protein Adsorption on Bioceramics.
Interface Focus 2012, 2 (3), 259–277. DOI:10.1098/rsfs.2012.0012.
(14) Yue, B. Biology of the Extracellular Matrix. *Journal of Glaucoma* **2014**, *23*. DOI:10.1097/ijg.0000000000000108.
(15) Sung, T.-C.; Wang, T.; Liu, Q.; Ling, Q.-D.; Subbiah, S. K.; Renuka, R. R.; Hsu, S.-T.; Umezawa, A.; Higuchi, A. Cell-Binding Peptides on the Material Surface Guide Stem Cell Fate of Adhesion, Proliferation and Differentiation. *Journal of Materials Chemistry B* **2023**, *11* (7), 1389–1415. DOI:10.1039/d2tb02601e.
(16) B. Sivaraman, R.A. Latour, The relationship between platelet adhesion on surfaces and the structure versus the amount of adsorbed fibrinogen, *Biomaterials*. 31 (2010) 832–839. doi:10.1016/j.biomaterials.2009.10.008.
(17) Lam, M.; Vayron, R.; Delille, R.; Migonney, V.; Falentin-Daudré, C. Influence of Poly(Styrene Sodium Sulfonate) Grafted Silicone Breast Implant's Surface on the Biological Response and Its Mechanical Properties. *Materials Today Communications* **2022**, *31*, 103318. DOI:10.1016/j.mtcomm.2022.103318.
(18) Chouirfa, H.; Evans, M. D.; Bean, P.; Saleh-Mghir, A.; Crémieux, A. C.; Castner, D. G.; Falentin- Daudré, C.; Migonney, V. Grafting of Bioactive Polymers with Various Architectures: A Versatile Tool for Preparing Antibacterial Infection and Biocompatible Surfaces. *ACS Applied Materials & Interfaces* **2018**, *10* (2), 1480–1491. DOI:10.1021/acsami.7b14283.
(19) Pereira, C.; Baumann, J.-S.; Humblot, V.; Falentin-Daudré, C. Biological Properties of Direct Grafting by Ultraviolet Irradiation of Vinyl Benzyl Phosphonic Acid onto Titanium Surfaces. *Reactive and Functional Polymers* **2022**, *173*, 105215. DOI:10.1016/j.reactfunctpolym.2022.105215.
(20) Aresti, A.; Aragoneses, J.; López-Valverde, N.; Suárez, A.; Aragoneses, J. M. Effectiveness of Biofunctionalization of Titanium Surfaces with Phosphonic Acid. *Biomedicines* **2021**, *9* (11), 1663. DOI:10.3390/biomedicines9111663.
(21) Mahjoubi, H.; Buck, E.; Manimunda, P.; Farivar, R.; Chromik, R.; Murshed, M.; Cerruti, M. Surface Phosphonation Enhances Hydroxyapatite Coating Adhesion on Polyetheretherketone and Its Osseointegration Potential. *Acta Biomaterialia* **2017**, *47*, 149–158. DOI:10.1016/j.actbio.2016.10.004.
(22) Wozniak, A.; Humblot, V.; Vayron, R.; Delille, R.; Falentin-Daudré, C. Simple UV-Grafting of Polyacrylic and Polymethacrylic Acid on Silicone Breast Implant Surfaces: Chemical and Mechanical Characterizations. *Coatings* **2023**, *13* (11), 1888. DOI:10.3390/coatings13111888.
(23) Chouirfa, H.; Migonney, V.; Falentin-Daudré, C. Grafting Bioactive Polymers onto Titanium Implants by UV Irradiation. *RSC Advances* **2016**, *6* (17), 13766–13771. DOI:10.1039/c5ra24497h.
(24) Li, Y.; Zhang, X.; Chen, W.; Liu, J.; Wang, H.; Zhou, Z.; Sun, Q. Surface Modification of Titanium Implants with Bioactive Polymer Coatings for Enhanced Osseointegration and Antibacterial Properties. Acta Biomater. 2024, 162, 209–222. DOI :10.1016/j.actbio.2023.12.024.
(25) Wang, Z.; Ma, X.; Wang, J.; Zhang, Y.; Chen, S.; Yu, L.; Wang, S.; Wang, X. Facile Synthesis of

Biocompatible Polymer Brushes on Titanium Surfaces via Surface-Initiated ATRP for Enhanced Osteoblast Adhesion. Adv. Mater. 2016, 28 (16), 3272–3278. DOI : 10.1002/adma.201504033.

(26) Abueva, C. D.; Jang, D.-W.; Padalhin, A.; Lee, B.-T. Phosphonate-Chitosan Functionalization of a Multi-Channel Hydroxyapatite Scaffold for Interfacial Implant-Bone Tissue Integration. *Journal of Materials Chemistry B* **2017**, *5*(6), 1293–1301. DOI:10.1039/c6tb03228a.

(27) Damiati, L. A.; Tsimbouri, M. P.; Hernandez, V.-L.; Jayawarna, V.; Ginty, M.; Childs, P.; Xiao, Y.; Burgess, K.; Wells, J.; Sprott, M. R.; Meek, R. M. D.; Li, P.; Oreffo, R. O. C.; Nobbs, A.; Ramage, G.; Su, B.; Salmeron-Sanchez, M.; Dalby, M. J. Materials-Driven Fibronectin Assembly on Nanoscale Topography Enhances Mesenchymal Stem Cell Adhesion, Protecting Cells from Bacterial Virulence Factors and Preventing Biofilm Formation. *Biomaterials* **2022**, *280*, 121263. DOI:10.1016/j.biomaterials.2021.121263.

(28) Parisi, L.; Ghezzi, B.; Bianchi, M. G.; Toffoli, A.; Rossi, F.; Bussolati, O.; Macaluso, G. M. Titanium Dental Implants Hydrophilicity Promotes Preferential Serum Fibronectin over Albumin Competitive Adsorption Modulating Early Cell Response. *Materials Science and Engineering: C* **2020**, *117*, 111307. DOI:10.1016/j.msec.2020.111307.

(29) Venault, A.; Wei, T.-C.; Shih, H.-L.; Yeh, C.-C.; Chinnathambi, A.; Alharbi, S. A.; Carretier, S.; Aimar, P.; Lai, J.-Y.; Chang, Y. Antifouling Pseudo-Zwitterionic Poly(Vinylidene Fluoride) Membranes with Efficient Mixed-Charge Surface Grafting via Glow Dielectric Barrier Discharge Plasma-Induced Copolymerization. *Journal of Membrane Science* **2016**, *516*, 13–25. DOI:10.1016/j.memsci.2016.05.044.

(30) Lam, M.; Moris, V.; Humblot, V.; Migonney, V.; Falentin-Daudré, C. A Simple Way to Graft a Bioactive Polymer – Polystyrene Sodium Sulfonate on Silicone Surfaces. Eur. Polym. J. 2020, 128, 109608.DOI: 10.1016/j.eurpolymj.2020.109608

(31) Kocen, R.; Gasik, M. Biomaterial Properties and Considerations in Designing Hydrogel Coatings for Medical Devices. *BioNanoSci.* **2012**, *2* (4), 249–257.DOI: 10.1007/s13758-012- 0048-4.

(32)(32) Pickup, M.; Novitskiy, S.; Moses, H. L. The Roles of TGFβ in the Tumour Microenvironment. *Oncogene* **2013**, *32* (17), 2225–2233. DOI: 10.1038/onc.2013.118.

(33) M. Pegueroles, C. Tonda-Turo, J.A. Planell, F.-J. Gil, C. Aparicio, Adsorption of fibronectin, fibrinogen, and albumin on tio2: Time-resolved kinetics, structural changes, and competition study, *Biointerphases*. 7 (2012). Doi:10.1007/s13758-012-0048-4.

(34) Felgueiras, H. P.; Evans, M. D. M.; Migonney, V. Contribution of Fibronectin and Vitronectin to the Adhesion and Morphology of MC3T3-E1 Osteoblastic Cells to Poly(Nass) Grafted TI6AL4V. *Acta Biomaterialia* **2015**, *28*, 225–233. DOI:10.1016/j.actbio.2015.09.030.

(35) Lam, M.; Falentin-Daudré, C. Characterization of Plasmatic Proteins Adsorption on Poly(Styrene Sodium Sulfonate) Functionalized Silicone Surfaces. *Biophysical Chemistry* **2022**, *285*, 106804. DOI:10.1016/j.bpc.2022.106804.

(36) Chai, H.; Zhang, Z. H.; Fang, J. Y.; She, C.; Geng, D. C.; Xu, W. Osteocytic Cells Exposed to Titanium Particles Increase Sclerostin Expression and Inhibit Osteoblastic Cell Differentiation Mostly via Direct Cell-to-Cell Contact. J. Cell. Mol. Med. 2022, 26 (15), 4371–4385.
DOI:10.1111/jcmm.17460

(37) Sinirlioglu, D.; Muftuoglu, A. E.; Bozkurt, A. Novel Composite Polymer Electrolyte Membranes Based on Poly(vinyl phosphonic acid) and Poly(5-(methacrylamido)tetrazole). Polym. Eng. Sci. 2015, 55 (2), 260–269. DOI: 10.1002/pen.23890

(38) Wang, F.; Zhang, H.; Yu, B.; Wang, S.; Shen, Y.; Cong, H. Review of the Research on Anti-Protein Fouling Coatings Materials. *Progress in Organic Coatings* **2020**, *147*, 105860. DOI:10.1016/j.porgcoat.2020.105860.

(39) Aramesh, M.; Shimoni, O.; Ostrikov, K.; Prawer, S.; Cervenka, J. Surface Charge Effects in Protein Adsorption on Nanodiamonds. *Nanoscale* **2015**, *7* (13), 5726–5736. DOI:10.1039/c5nr00250h.

(40) (40)ISO10993-1:2018. https://www.iso.org/standard/68936.html (accessed 2025-01-09).Keselowsky, B. G.; Collard, D. M.; García, A. J. Surface Chemistry Modulates Fibronectin Conformation and Directs Integrin Binding and Specificity to Control Cell Adhesion. *Journal of Biomedical Materials Research Part A* **2003**, *66A* (2), 247–259. DOI:10.1002/jbm.a.10537.

(41) Suneetha, M.; Kim, H.; Han, S. S. Bone-like Apatite Formation in Biocompatible Phosphate- Crosslinked Bacterial Cellulose-Based Hydrogels for Bone Tissue Engineering Applications. *International Journal of Biological Macromolecules* **2024**, *256*, 128364. DOI:10.1016/j.ijbiomac.2023.128364.

(42) Serguienko, A.; Wang, M. Y.; Myklebost, O. Real-Time Vital Mineralization Detection and Quantification during in Vitro Osteoblast Differentiation. *Biological Procedures Online* **2018**, *20* (1). DOI:10.1186/s12575-018-0079-4.

(43) Felgueiras, H. P.; Ben Aissa, I.; Evans, M. D. M.; Migonney, V. Contributions of Adhesive Proteins to the Cellular and Bacterial Response to Surfaces Treated with Bioactive Polymers: Case of Poly(sodium Styrene Sulfonate) Grafted Titanium Surfaces. J. Mater. Sci.: Mater.
Med. 2015, 26 (11), 261. DOI: 10.1007/s10856-015-5596-y

(44) Ribeiro, M.; Monteiro, F. J.; Ferraz, M. P. Infection of Orthopedic Implants with Emphasis on Bacterial Adhesion Process and Techniques Used in Studying Bacterial-Material Interactions. *Biomatter* **2012**, *2* (4), 176–194. DOI:10.4161/biom.22905.

(45) Ferraris, S.; Spriano, S. Antibacterial Titanium Surfaces for Medical Implants. *Materials Science and Engineering: C* **2016**, *61*, 965–978. DOI:10.1016/j.msec.2015.12.062.

(46) Henderson, B.; Nair, S.; Pallas, J.; Williams, M. A. Fibronectin: A Multidomain Host Adhesin Targeted by Bacterial Fibronectin-Binding Proteins. *FEMS Microbiology Reviews* **2011**, *35* (1), 147–200. DOI:10.1111/j.1574-6976.2010.00243.x.

(47) Liamas, E.; Black, R. A.; Mulheran, P. A.; Tampé, R.; Wieneke, R.; Thomas, O. R.; Zhang, Z. J. Probing Fibronectin Adsorption on Chemically Defined Surfaces by Means of Single Molecule Force Microscopy. *Scientific Reports* **2020**, *10* (1). DOI:10.1038/s41598-020-72617-z.

(48) Vazquez, V.; Liang, X.; Horndahl, J. K.; Ganesh, V. K.; Smeds, E.; Foster, T. J.; Hook, M.

Fibrinogen Is a Ligand for the Staphylococcus Aureus Microbial Surface Components Recognizing Adhesive Matrix Molecules (MSCRAMM) Bone Sialoprotein-Binding Protein (BBP). *Journal of Biological Chemistry* **2011**, *286* (34), 29797–29805. DOI:10.1074/jbc.m110.214981.